Benha Journal of Applied Sciences (BJAS) print: ISSN 2356–9751
Vol. (9) Issue (5) (2024), (23-30) online: ISSN 2356–976x
http://bjas.bu.edu.eg

Solution of fractional order chaotic oscillator system

Asmaa A. Salama*, Mourad S. Semary and D.A. Hammad
Basic Engineering sciences Department, Benha faculty of engineering, Benha University, Benha 13512, Egypt
E-mail: asmaa.salama@bhit.bu.edu.eg

Abstract

Mathematical and scientific fields of study that are interdisciplinary include chaos theory. chaos theory explains how there is sensitive dependence on initial conditions, meaning that small change in one state of a deterministic nonlinear system can lead to large differences in a later state. The nonvolatile meminductor and memcapacitor models are used to design a nonlinear chaotic oscillating circuit. There is a system of equations derived from chaotic oscillator which is called chaotic oscillator system. The predictor corrector method is presented by using the help of explicit Adams method and implicit Adams method. The predictor corrector method is proposed for solving a chaotic system of differential equations. A new iterative method is proved using characteristics and some fundamental definition of fractional calculus. The new iterative method is used for solving the chaotic system of fractional differential equations. The domain is divided into smaller domains, and an approximative solution for the whole domain can be obtained by solving iteratively. The simulation results are presented. Output chaotic phases are shown in figures. An analysis of the chaotic oscillator system ’s stability is conducted.

Keywords: chaotic oscillator, Predictor corrector method, Fractional calculus

1. Introduction

A nonlinear circuit built using models of nonvolatile meminductor, memcapacitor and memristor is called a chaotic oscillator [1-20]. chaotic oscillator’s application areas are synchronization approach which depends on initial setting and communication encryption. In this study, the chaotic oscillator system [21-23] is taken the following form.

$$\begin{aligned} D_a^{\beta_1} p(t) &= P(t) \\ D_a^{\beta_2} q(t) &= Q(t) \\ &\vdots \\ D_a^{\beta_l} u(t) &= U(t) \end{aligned} \qquad (1.1)$$

First, the predictor corrector method (PCM) [24–26] is a class of algorithms designed to integrate ordinary differential equations (ODEs) and find an unknown function that satisfies a given differential equation. PCM is presented using the help of two methods (explicit Adams-Bashforth method and Adams Moulton implicit multistep-method). The combination between explicit method to predict and implicit method is to improve predict value. The Explicit Adams-Bashforth method is used to prove predict value. The implicit multistep method of Adams Moulton is used to prove the correct value.

Second, fractional order differential equations are frequently encountered in a variety of applications so, they have been the subject of numerous studies. Several scientific domains have utilized fractional numerical calculus [27-30]. Derivatives and integrals of any order, including distributed, constant, and variable are studied in fractional calculus, so called fractional differential equations (FDEs) [31-34]. The paper presents a new iterative technique for solving fractional differential system. The new iterative method depends on dividing the domain into smaller domains and solving each subdomain iteratively. Some fundamental definitions of FDE are presented. Caputo’s definition [35,36] has a better initial condition, so it is more appropriate. The fractional derivatives are characterized by the Caputo sense. After that, the system's stability analysis is presented.

Many researchers used ode45 for the solution of nonlinear ODE system as in [21, 37] and references therein. Also, many researchers used Grunwald Letnikov definition (GLD) for the solution of nonlinear FDE system as in [35] and references therein. The first main objective of this work is solving chaotic system (ODE) using the PCM. The chaotic system has taken its equation as FDEs. The second main objective is solving initial value FDEs0 using a new iterative technique.

This paper is organized as follows: In **Section 2**, PCM and a new iterative method are presented in detail. **Section 3** contains some numerical results for solving chaotic oscillator system using PCM and numerical results for solving the fractional order of chaotic oscillator system using an iterative method. In **Section 4**, we study the stability analysis of the system. The Routh Hurwitz rule is used to check the stability analysis of the system.

2. Methods description for ODEs and FDEs

Through this section, we present PCM and a new iterative method. We use PCM to solve chaotic system of ODEs and a new iterative method to solve chaotic system of FDEs.

2.1. Predictor corrector method

PCM uses a suitable employs an appropriate combination of explicit and implicit techniques to achieve better converge. PCM uses the fourth order Adam-Bashforth method as predictor. By using the explicit Adams-Bashforth method, also known as the predict value, we can obtain the first approximation. We use one iteration of the Adams-Moulton implicit to obtain the correct value.

The predicted value is.

$$\begin{aligned} p^{*}_{n+1} &= p_n + \frac{h}{24}(55P_n - 59P_{n-1} + 37P_{n-2} - 9P_{n-3}) \\ q^{*}_{n+1} &= q_n + \frac{h}{24}(55Q_n - 59Q_{n-1} + 37Q_{n-2} - 9Q_{n-3}) \\ &\vdots \\ u^{*}_{n+1} &= u_n + \frac{h}{24}(55U_n - 59U_{n-1} + 37U_{n-2} - 9U_{n-3}) \end{aligned} \tag{2.1}$$

and correct value is

$$\begin{aligned} p_{n+1} &= p_n + \frac{h}{24}(9P_{n+1} + 19P_n - 5P_{n-1} + P_{n+2}) \\ q_{n+1} &= q_n + \frac{h}{24}(9Q_{n+1} + 19Q_n - 5Q_{n-1} + Q_{n+2}) \\ &\vdots \\ u_{n+1} &= u_n + \frac{h}{24}(9U_{n+1} + 19U_n - 5U_{n-1} + U_{n+2}) \end{aligned} \tag{2.2}$$

The first four values of each output variable need to be known, so we can calculate them using Rung-Kutta of second order (RK-2) [38-40].

2.2. Iterative method for solving fractional initial value problems.

We give an overview of how fractional initial value problems (FIVPs) can be solved numerically [41-49]. To solve the problem iteratively and get an approximation for the entire domain, we divided the domain into subdomains. This method justification is shown on the system of the form Eq. (1.1).

At $0 < \beta_i \le 1$ for $i = 1, 2, ..., l$ with initial values

$$\begin{aligned} p(a) &= \alpha_1 \\ q(a) &= \alpha_2 \\ &\vdots \\ u(a) &= \alpha_l \end{aligned} \tag{2.3}$$

where $\alpha_1, \alpha_2, \cdots, \alpha_l \in R$.

A few basic definitions and features of fractional calculus theory are necessary to understand:

1. A left-sided Riemann-Liouville fractional integral operator of order β is defined as
$$J_a^{\beta} x(\mathrm{t}) = \frac{1}{\Gamma(\beta)} \int_a^t (\mathrm{t} - \tau)^{\beta - 1} x(\tau) \mathrm{d}\tau \quad , \quad \beta \in R, \tag{2.4}$$
Where $t \in [a, T]$ and Γ is described as the gamma function of Euler by $\Gamma(\beta) = \int_0^{\infty} \mathrm{s}^{\beta-1} e^{-\mathrm{s}} \mathrm{ds}$
2. The left-sided Caputo fractional derivatives operator [50,51] is defined as follows.
$$D_a^{\beta} x(t) = J_a^{m-\beta} x^{(m)}(t) = \frac{1}{\Gamma(m-\beta)} \int_a^t (t-\tau)^{m-\beta-1} x^{(m)}(\tau) d\tau, \tag{2.5}$$
for $\beta \in R, \mathrm{m} = \lceil \beta \rceil$ where m is the ceiling of β ,and $t \in [a, T]$.
3. for $t \in [a, T]$ we have
$$\begin{aligned} D_a^{\beta} J_a^{\beta} x(t) &= x(t). \\ J_a^{\beta} D_a^{\beta} x(t) &= x(t) - \sum_{K=0}^{m-1} x^{(k)}(a) \frac{t^k}{k!} \end{aligned} \tag{2.6}$$

N−subintervals are created within the domain $[a,T]$ using the grid points $t_n = a + nh$, $n = 0,1,....,N$ where h indicates a uniform step size $h = (T-a)/N$. Writing the domain in one way is $M = \bigcup_{n=1}^{N} M_n$ where $M_n = [t_{n-1}, t_n]$. Since $\beta \in (0,\ 1]$, we consider that at the nodes t_{n-1},the solution is continuous.

For $t \in M_n$ Eq. (1.1) convert to

$$D_{t_{n-1}}^{\beta_1} p_n(t) = P(t, p_n(t)),\quad p_n(t_{n-1}) = \begin{cases} p_{n-1}(t_{n-1}), & n>1 \\ \alpha_1, & n=1 \end{cases}.$$
$$D_{t_{n-1}}^{\beta_2} q_n(t) = Q(t, q_n(t)),\quad q_n(t_{n-1}) = \begin{cases} q_{n-1}(t_{n-1}), & n>1 \\ \alpha_2, & n=1 \end{cases}.$$
$$\vdots$$
$$D_{t_{n-1}}^{\beta_l} u_n(t) = U(t, u_n(t)),\quad u_n(t_{n-1}) = \begin{cases} u_{n-1}(t_{n-1}), & n>1 \\ \alpha_l, & n=1 \end{cases}. \quad (2.7)$$

by taking $J_{t_{n-1}}^{\beta_i}$ where $i = 1,2,\ldots,l$ for both sides

$$J_{t_{n-1}}^{\beta_1} D_{t_{n-1}}^{\beta_1} p(t) = J_{t_{n-1}}^{\beta_1} P(t, p(t))$$
$$J_{t_{n-1}}^{\beta_2} D_{t_{n-1}}^{\beta_2} q(t) = J_{t_{n-1}}^{\beta_2} Q(t, q(t))$$
$$\vdots$$
$$J_{t_{n-1}}^{\beta_l} D_{t_{n-1}}^{\beta_l} u(t) = J_{t_{n-1}}^{\beta_l} U(t, u(t)) \quad (2.8)$$

using Eq. (2.4) and Eq. (2.6) the output for each side will be.

$$p_n(t) - p_n(t_{n-1}) = \frac{1}{\Gamma(\beta_1)} \int_{t_{n-1}}^{t_n} (t-\tau)^{\beta_1 - 1} P(\tau, p_n(\tau)) d\tau$$
$$q_n(t) - q_n(t_{n-1}) = \frac{1}{\Gamma(\beta_2)} \int_{t_{n-1}}^{t_n} (t-\tau)^{\beta_2 - 1} Q(\tau, p_n(\tau)) d\tau$$
$$\vdots$$
$$u_n(t) - u_n(t_{n-1}) = \frac{1}{\Gamma(\beta_l)} \int_{t_{n-1}}^{t_n} (t-\tau)^{\beta_l - 1} U(\tau, u_n(\tau)) d\tau \quad (2.9)$$

At node t_{n-1}, the result is obtained by applying the continuity condition ,i.e., $x_n(t_{n-1}) = x_{n-1}(t_{n-1})$ and for $t \in M_n$ Eq. (2.9) on sub-domain M_n is equivalent to the following integral equation:

$$p_n(t) = p_{n-1}(t_{n-1}) + \frac{1}{\Gamma(\beta_1)} \int_{t_{n-1}}^{t} (t-\tau)^{\beta_1 - 1} P(\tau, p_n(\tau)) d\tau$$
$$q_n(t) = q_{n-1}(t_{n-1}) + \frac{1}{\Gamma(\beta_2)} \int_{t_{n-1}}^{t} (t-\tau)^{\beta_2 - 1} Q(\tau, q_n(\tau)) d\tau \quad (2.10)$$
$$\vdots$$
$$u_n(t) = u_{n-1}(t_{n-1}) + \frac{1}{\Gamma(\beta_l)} \int_{t_{n-1}}^{t} (t-\tau)^{\beta_l - 1} U(\tau, u_n(\tau)) d\tau$$

by approximate the function.

$$P(\tau, p_n(\tau)) \approx P(t_{n-1}, p_{n-1}(t_{n-1}))$$
$$Q(\tau, q_n(\tau)) \approx Q(t_{n-1}, q_{n-1}(t_{n-1})) \quad (2.11)$$
$$\vdots$$
$$U(\tau, u_n(\tau)) \approx U(t_{n-1}, u_{n-1}(t_{n-1}))$$

at point $t = t_{n-1}$. After integration Eq. (2.10) convert to

$$p_n(t) = p_{n-1}(t_{n-1}) + \frac{P(t_{n-1}, p_{n-1}(t_{n-1}))}{\Gamma(\beta_1)} (t - t_{n-1})^{\beta_1}$$
$$q_n(t) = q_{n-1}(t_{n-1}) + \frac{Q(t_{n-1}, q_{n-1}(t_{n-1}))}{\Gamma(\beta_2)} (t - t_{n-1})^{\beta_2} \quad (2.12)$$
$$\vdots$$
$$u_n(t) = u_{n-1}(t_{n-1}) + \frac{U(t_{n-1}, u_{n-1}(t_{n-1}))}{\Gamma(\beta_l)} (t - t_{n-1})^{\beta_l}$$

by replacing t by t_n Eq. (2.12) can be solved using explicit Euler method.

3. Results and discussions

Case 1:

A chaotic oscillator circuit [52,53] was presented in [13] and a chaotic system Eq. (3.1) is produced from chaotic oscillator circuit. In this example, we consider $\beta = 1$, so the system is written as

$$\frac{dp(t)}{dt} = g_1 r(t) + g_2 r(t)s(t) - p(t)$$
$$\frac{dq(t)}{dt} = g_3 q(t) + g_4 q(t)u^2(t) - g_5 r(t) - g_6 r(t)s(t)$$
$$\frac{dr(t)}{dt} = g_7 q(t) + g_8 q(t)u^2(t) - g_9 p(t) \quad (3.1)$$
$$\frac{ds(t)}{dt} = g_{10} r(t)$$
$$\frac{du(t)}{dt} = g_{11} q(t)$$

with parameters:

$g_1 = 1.73, g_2 = -2.04, g_3 = 0.46, g_4 = 0.04,$
$g_5 = 0.67, g_6 = 0.19, g_7 = 0.48, g_8 = 0.52$
$and\ g_9 = g_{10} = g_{11} = .21$

and initial conditions are $p(0) = 0.2, q(0) = 0.5, r(0) = 0.45, s(0) = 0.1$ $and\ u(0)$=.5

The time step is $h_t = .005$ and the time of simulation $T = 1000$, so the number of points $N = T / h_t$.

Step one: we calculate the four initial values using RK-2 and the output is presented in Table 1.

Step two: we get the predict and correct values for each variable.

Let

$$A = g_1 r(t) + g_2 r(t)s(t) - p(t)$$
$$B = g_3 q(t) + g_4 q(t)u^2(t) - g_5 r(t) - g_6 r(t)s(t)$$
$$C = g_7 q(t) + g_8 q(t)u^2(t) - g_9 p(t) \quad (3.2)$$
$$D = g_{10} r(t)$$
$$E = g_{11} q(t)$$

predict values are.

$$p^*_{n+1} = p_n + \frac{h_t}{24}(55A_n - 59A_{n-1} + 37A_{n-2} - 9A_{n-3})$$
$$q^*_{n+1} = q_n + \frac{h_t}{24}(55B_n - 59B_{n-1} + 37B_{n-2} - 9B_{n-3})$$
$$r^*_{n+1} = r_n + \frac{h_t}{24}(55C_n - 59C_{n-1} + 37C_{n-2} - 9C_{n-3}) \quad (3.3)$$
$$s^*_{n+1} = s_n + \frac{h_t}{24}(55D_n - 59D_{n-1} + 37D_{n-2} - 9D_{n-3})$$
$$u^*_{n+1} = u_n + \frac{h_t}{24}(55E_n - 59E_{n-1} + 37E_{n-2} - 9E_{n-3})$$

and correct values are.

$$p_{n+1} = p_n + \frac{h_t}{24}(9A_{n+1} + 19A_n - 5A_{n-1} + A_{n+2})$$
$$q_{n+1} = q_n + \frac{h_t}{24}(9B_{n+1} + 19B_n - 5B_{n-1} + B_{n+2})$$
$$r_{n+1} = r_n + \frac{h_t}{24}(9C_{n+1} + 19C_n - 5C_{n-1} + C_{n+2}) \quad (3.4)$$
$$s_{n+1} = s_n + \frac{h_t}{24}(9D_{n+1} + 19D_n - 5D_{n-1} + D_{n+2})$$
$$u_{n+1} = u_n + \frac{h_t}{24}(9E_{n+1} + 19E_n - 5E_{n-1} + E_{n+2})$$

The chaotic phase between $p-q, q-s, r-u, r-s, s-u\ and\ p-s$ are shown in Figures (1-6), respectively.

Adam-Moulton implicit method give better results than explicit Adams-Bashforth for the same order. The combination between explicit method to predict and implicit method to improve the results. The same system of ordinary differential equation is solved using ode45 in [21]. Predictor corrector output has greater accuracy than ode45, so it is better to use PCM than ode45.

Table (1) the first four values of outputs using RK-2

p	q	r	s	u
0.2000	0.5000	0.4500	0.1000	0.5000
0.4110	0.4381	0.5623	0.1517	0.5486
0.5658	0.3216	0.6338	0.2131	0.5882
0.6516	0.1528	0.6507	0.2792	0.6134

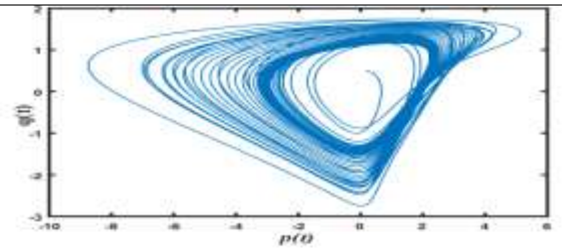

Fig. (1) chaotic phase between $p-q$

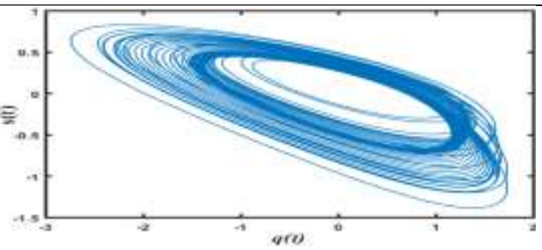

Fig. (2) chaotic phase between $q-s$

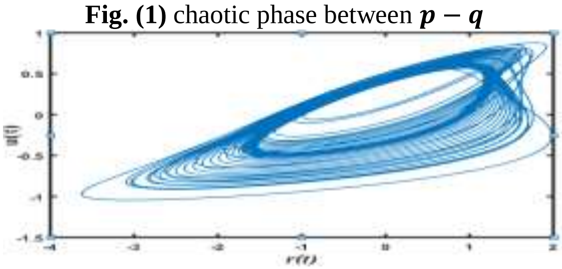

Fig. (3) chaotic phase between $r-u$

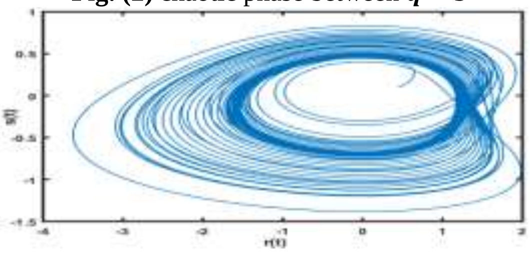

Fig. (4) chaotic phase between $r-s$

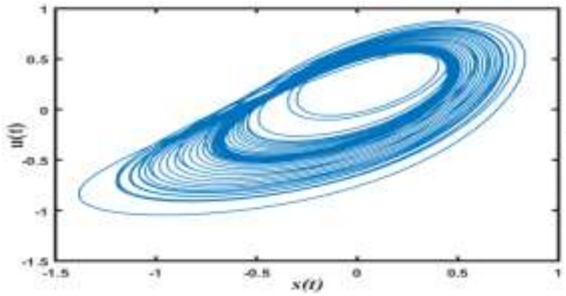

Fig. (5) chaotic phase between $s-u$

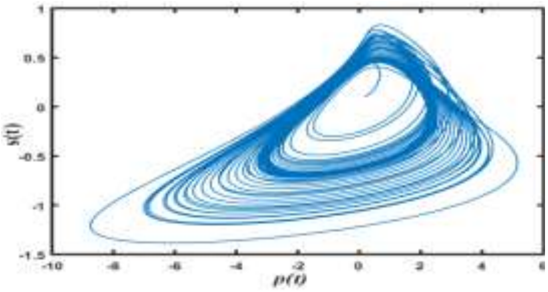

Fig. (6) chaotic phase between $p-s$

Case 2:

For the same **Case 1** mentioned above we have the same system of equations. Now, we need to solve it as a system of FDE mentioned in [49]. The value for $0<\beta\le 1$ and with the same parameter and initial values in **Case 1**. Instead of system in Eq. (3.1), we get the following set of FDEs .

$$
\begin{aligned}
&{}_aD_T^{\beta_1} p(t) = g_1 r(t) + \\
&g_2 r(t)s(t) - p(t) \\
&{}_aD_T^{\beta_2} q(t) = g_3 q(t) + g_4 q(t)u^2(t) \\
&-g_5 r(t) - g_6 r(t)s(t) \\
&{}_aD_T^{\beta_3} r(t) = g_7 q(t) + \\
&g_8 q(t)u^2(t) - g_9 p(t) \\
&{}_aD_T^{\beta_4} s(t) = g_{10} r(t) \\
&{}_aD_T^{\beta_5} u(t) = g_{11} q(t)
\end{aligned}
\tag{3.5}
$$

where $\beta_1 = .9, \beta_2 = \beta_3 = \beta_4 = \beta_5 = 1$. **Case 2** is different from **Case 1** in h_t. In **Case 1** $h_t = .005$ and in this **Case 2** $h_t = .0005$. Iterative method works in wide range, so we minimize h_t. If we apply iterative method described in **Section 2**, we can get

$$A\left(t_{n-1}, p_{(n-1)}\left(t_{n-1}\right)\right) = g_1 r_{n-1}(t_{n-1}) + g_2 r_{n-1}(t_{n-1}) s_{n-1}(t_{n-1}) - p_{n-1}(t_{n-1})$$

$$B\left(t_{n-1}, q_{(n-1)}\left(t_{n-1}\right)\right) = g_3 q_{n-1}(t_{n-1}) + g_4 q_{n-1}(t_{n-1}) u_{n-1}{}^2(t_{n-1}) - g_5 r_{n-1}(t_{n-1}) - g_6 r_{n-1}(t_{n-1}) s_{n-1}(t_{n-1})$$

$$C\left(t_{n-1}, r_{(n-1)}\left(t_{n-1}\right)\right) = g_7 q_{n-1}(t_{n-1}) + g_8 q_{n-1}(t_{n-1}) u_{n-1}{}^2(t_{n-1}) - g_9 p_{n-1}(t_{n-1})$$

$$D\left(t_{n-1}, s_{(n-1)}\left(t_{n-1}\right)\right) = g_{10} r_{n-1}(t_{n-1})$$

$$E\left(t_{n-1}, u_{(n-1)}\left(t_{n-1}\right)\right) = g_{11} q_{n-1}(t_{n-1})$$

and hence, we obtain.

$$p_n = p_{n-1} + \frac{h_t^{\beta_1}}{\Gamma(\beta_1+2)} * (\beta_1 A\left(t_{n-1}, p_{n-1}\left(t_{n-1}\right)\right) + A\left(t_n, p_n\left(t_n\right)\right))$$

$$q_n = q_{n-1} + \frac{h_t^{\beta_2}}{\Gamma(\beta_2+2)} * (\beta_2 B\left(t_{n-1}, q_{n-1}\left(t_{n-1}\right)\right) + B\left(t_n, q_n\left(t_n\right)\right))$$

$$r_n = r_{n-1} + \frac{h_t^{\beta_3}}{\Gamma(\beta_3+2)} (\beta_3 C\left(t_{n-1}, r_{n-1}\left(t_{n-1}\right)\right) + C\left(t_n, r_n\left(t_n\right)\right))$$

$$s_n = s_{n-1} + \frac{h_t^{\beta_4}}{\Gamma(\beta_4+2)} (\beta_4 D\left(t_{n-1}, s_{n-1}\left(t_{n-1}\right)\right) + D\left(t_n, s_n\left(t_n\right)\right))$$

$$u_n = u_{n-1} + \frac{h_t^{\beta_5}}{\Gamma(\beta_5+2)} * (\beta_5 E\left(t_{n-1}, u_{n-1}\left(t_{n-1}\right)\right) + E\left(t_n, u_n\left(t_n\right)\right))$$

The chaotic phase between $p-q, p-s, s-u, y-s,$ $\mathrm{r}-u$ *and* $\mathrm{r}-s$ are shown in Figures (7-12), respectively.

We use small h_t to get better results as iterative method works correctly for wide range. The same system of fractional differential equation is solved using Grunwald-Letnikov definition (GLD) and output results is shown in [49]

4. Stability analysis of the system

Let

(3.6) $$\frac{dp}{dt} = 0, \frac{dq}{dt} = 0, \frac{dr}{dt} = 0, \frac{ds}{dt} = 0, \frac{du}{dt} = 0$$

in Eq. (3.3), the system will be

$$\begin{aligned} & g_1 r(t) + g_2 r(t) s(t) - p(t) = 0 \\ & g_3 q(t) + g_4 q(t) u^2(t) - g_5 r(t) - g_6 r(t) s(t) = 0 \\ & g_7 q(t) + g_8 q(t) u^2(t) - g_9 p(t) = 0 \\ & g_{10} r(t) = 0 \\ & g_{11} q(t) = 0 \end{aligned} \tag{4.1}$$

The system's equilibrium points can set as $L(0,0,0,v_1,v_2)$, this suggests that the number of equilibrium points in this system are infinite. According to the system in Eq. (3.1), The system 's jacobine matrix expressed as

$$J_C = \begin{pmatrix} -1 & 0 & g_1+g_2 v_1 & 0 & 0 \\ 0 & g_3+g_4 v_2^2 & -g_5-g_6 v_1 & 0 & 0 \\ -g_9 & g_7+g_8 v_2^2 & 0 & 0 & 0 \\ 0 & 0 & g_9 & 0 & 0 \\ 0 & g_9 & 0 & 0 & 0 \end{pmatrix} \tag{4.2}$$

And the characteristic equation can be calculated as follows.

(3.7)

$$\lambda^5 - (x_2-1)\lambda^4 + (x_1 x_3 - x_2 - x_4 x_5)\lambda^3 - (x_1 x_2 x_3 + x_4 x_5)\lambda^2 = 0 \tag{4.3}$$

Where $x_1 = g_1 + g_2 v_1$, $x_2 = g_3 + g_4 v_2^2$, $x_3 = g_9$, $x_4 = -g_5 - g_6 v_1$, $x_5 = g_7 + g_8 v_2^2$.

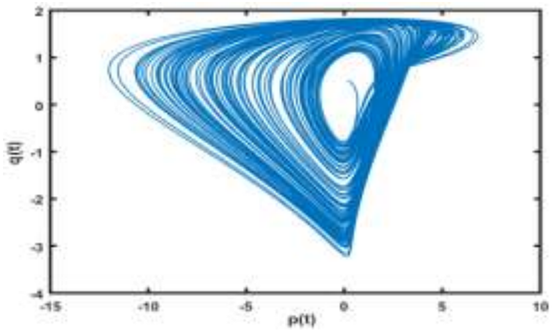

Fig. (7) chaotic phase between $\boldsymbol{p-q}$

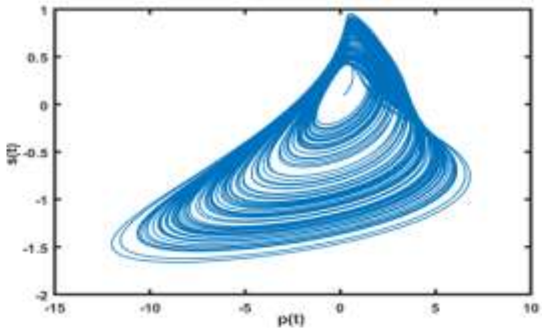

Fig. (8) chaotic phase between $\boldsymbol{p-s}$

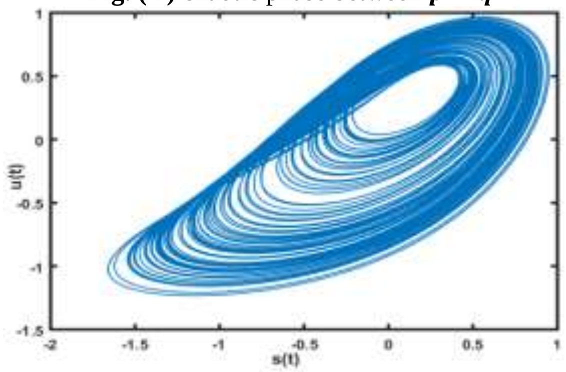

Fig. (9) chaotic phase between $\boldsymbol{s-u}$

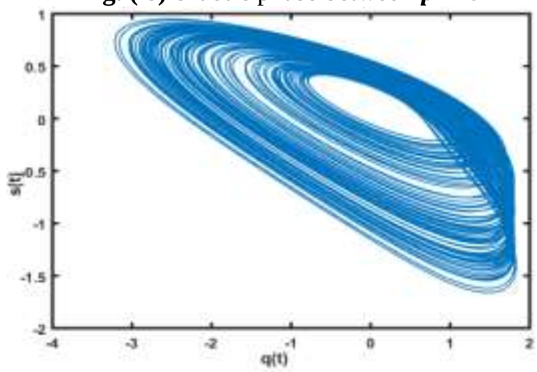

Fig. (10) chaotic phase between $\boldsymbol{q-s}$

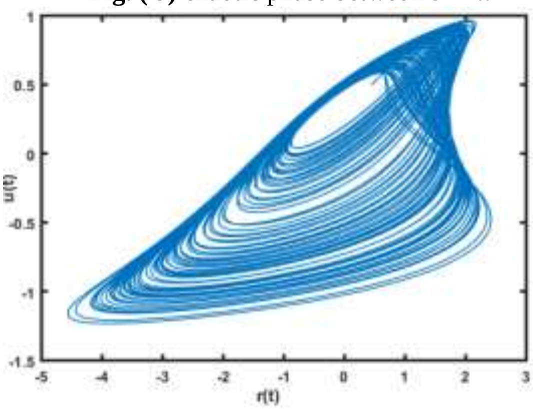

Fig. (11) chaotic phase between $\boldsymbol{r-u}$

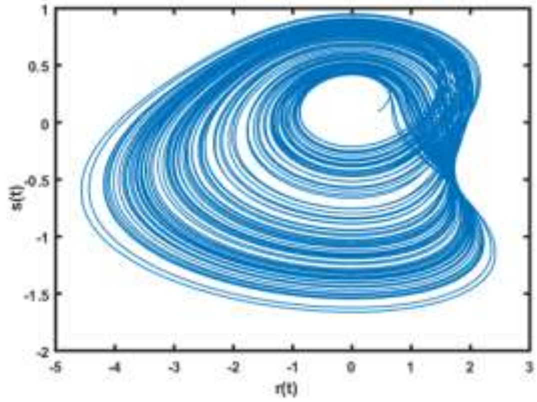

Fig. (12) chaotic phase between $\boldsymbol{r-s}$

The Routh Hurwitz rule states that, if $d_1=-x_2+1, d_2=(x_2-x_2^2-x_1x_3-x_2x_4x_5)/(x_2-1)$, $d_3=-x_4x_5-x_1x_2x_3$ are all positive, the system 's eigenvalues will all be negative, and the system will be stable. Therefore, for this system to function in a chaotic state, at least one of its eigenvalues needs to be positive. This implies that d_1, d_2 *and* d_3 shouldn't all be positive. Because of this, we could set L like $L(0,0,0,0,4)$ with the same parameters. We get $d_1=-.1<0$ which indicate that, at any equilibrium point, this system is unstable and the ability to create chaos within the system.

5. Conclusion

PCM is used to solve ODEs of chaotic system. Matlab is the software was used for simulation. Output results from PCM are more accurate than results of ode45. The same chaotic system of equations is solved as FDEs. Iterative method is used to solve the chaotic system of FDEs. The iterative method depends on splitting domain into small domains. The iterative method deals with FDEs with large domains, so it works correctly at small step size. Studying stability analysis of the system assure that the system is unstable. Other dynamical properties and a memory effect are detected by applying fractional order derivative to the mathematical model of the oscillator elements. Additionally, the derivative orders give us an increased degree of freedom.

References

[1] Chen, J. J., Yan, D. W., Duan, S. K., & Wang, L. D. (2020). Memristor-based

hyper-chaotic circuit for image encryption. Chinese Physics B, 29(11), 110504.

[2] Chen, X., Hassan, Y. A., Huang, X., Li, J., Hu, H., & Yue, J. (2023). Biocompatible AlOOH-based memristor with biomimicking synaptic functions for artificial nociceptor applications. Ceramics International.

[3] Demirkol, A. S., Ascoli, A., Messaris, I., & Tetzlaff, R. (2022). Pattern formation dynamics in a Memristor Cellular Nonlinear Network structure with a numerically stable VO2 memristor model. Japanese Journal of Applied Physics, 61(SM), SM0807.

[4] Wu, W., & Deng, N. (2017). Memristor interpretations based on constitutive relations. Journal of Semiconductors, 38(10), 104005.

[5] Zhong, W. M., Luo, C. L., Tang, X. G., Lu, X. B., & Dai, J. Y. (2023). Dynamic FET-based memristor with relaxor antiferroelectric HfO2 gate dielectric for fast reservoir computing. Materials Today Nano, 100357.

[6] Petráš, I., & Terpák, J. (2019). Fractional calculus as a simple tool for modeling and analysis of long memory process in industry. Mathematics, 7(6), 511.

[7] Chen, Q., Li, B., Yin, W., Jiang, X., & Chen, X. (2023). Bifurcation, chaos and fixed-time synchronization of memristor cellular neural networks. Chaos, Solitons & Fractals, 171, 113440.

[8] Li, C., & Sprott, J. C. (2016). Variable-boostable chaotic flows. Optik, 127(22), 10389-10398.

[9] Gao, C., Li, T., Cao, X., Liu, N., & Li, Q. (2021, March). Identification circuit based on memristor. In Journal of Physics: Conference Series (Vol. 1827, No. 1, p. 012007). IOP Publishing.

[10] Liu, X., Zou, L., Huang, C., Bai, N., Xue, K., Sun, H., & Miao, X. (2022, October). Analog Memristor-Based Dynamic Programmable Analog Filter. In Journal of Physics: Conference Series (Vol. 2356, No. 1, p. 012008). IOP Publishing.

[11] Shinde, S. S., & Dongle, T. D. (2015). Modelling of nanostructured TiO2-based memristors. Journal of Semiconductors, 36(3), 034001.

[12] Su, C. (2022, December). Dynamic Analysis and Chaotic Suppression of Cuk Converter under Memristor Load. In Journal of Physics: Conference Series (Vol. 2383, No. 1, p. 012046). IOP Publishing.

[13] Dai, Y., Zou, J., Feng, Z., Li, X., Wang, X., Hu, G., ... & Wu, Z. (2022). Modeling of a diffusive memristor based on the DT-FNT mechanism transition. Semiconductor Science and Technology, 37(9), 095001.

[14] Wang, F., Chen, K., Yi, X., Lin, Y., & Zhuang, S. (2023). A study on sodium alginate based memristor: From typical to self-rectifying. Materials Letters, 338, 134037.

[15] Yang, L., Ding, Z., & Zeng, Z. (2023). Memristor crossbar-based Pavlov associative memory network for dynamic information correlation. AEU-International Journal of Electronics and Communications, 159, 154472.

[16] Han, X., Bi, X., Sun, B., Ren, L., & Xiong, L. (2022). Dynamical analysis of two-dimensional memristor cosine map. Frontiers in Physics, 10, 401.

[17] Huang, L., Yu, H., Chen, C., Peng, J., Diao, J., Nie, H., ... & Liu, H. (2021). A training strategy for improving the robustness of memristor-based binarized convolutional neural networks. Semiconductor Science and Technology, 37(1), 015013.

[18] Laskaridis, L., Volos, C., Munoz-Pacheco, J., & Stouboulos, I. (2023). Study of the dynamical behavior of an Ikeda-based map with a discrete memristor. Integration, 89, 168-177.

[19] Lin, R., Shi, G., Qiao, F., Wang, C., & Wu, S. (2023). Research progress and applications of memristor emulator circuits. Microelectronics Journal, 105702.

[20] Ma, D., Hu, Y., Xu, N., Huang, C., Yang, B., Qiu, S., ... & Fang, L. (2021, July). Logics execution in a multi-layers memristor array. In Journal of Physics: Conference Series (Vol. 1976, No. 1, p. 012079). IOP Publishing.

[21] Wang, X., Yu, J., Jin, C., Iu, H. H. C., & Yu, S. (2019). Chaotic oscillator based on memcapacitor and meminductor. Nonlinear Dynamics, 96, 161-173.

[22] Yuan, F., & Li, Y. (2019). A chaotic circuit constructed by a memristor, a memcapacitor and a meminductor. Chaos: An Interdisciplinary Journal of Nonlinear Science, 29(10).

[23] Yuan, F., Wang, G., & Wang, X. (2017). Chaotic oscillator containing memcapacitor and meminductor and its dimensionality

reduction analysis. Chaos: An Interdisciplinary Journal of Nonlinear Science, 27(3).

[24] Deng, W. (2007). Short memory principle and a predictor–corrector approach for fractional differential equations. Journal of Computational and Applied Mathematics, 206(1), 174-188.

[25] Ghrist, M. L., Fornberg, B., & Reeger, J. A. (2015). Stability ordinates of Adams predictor-corrector methods. BIT Numerical Mathematics, 55, 733-750.

[26] Diethelm, K., Ford, N. J., & Freed, A. D. (2002). A predictor-corrector approach for the numerical solution of fractional differential equations. Nonlinear Dynamics, 29, 3-22.

[27] Kilbas, A. A., Srivastava, H. M., & Trujillo, J. J. (2006). Theory and applications of fractional differential equations (Vol. 204).

[28] Ata, E., & Kıymaz, I. O. (2023). New generalized Mellin transform and applications to partial and fractional differential equations. International Journal of Mathematics and Computer in Engineering, 1(1), 45-66.

[29] Abbas, S., Benchohra, M., Lazreg, J. E., Nieto, J. J., & Zhou, Y. (2023). Fractional differential equations and inclusions: classical and advanced topics.

[30] Khan, H., Alzabut, J., & Gulzar, H. (2023). Existence of solutions for hybrid modified ABC-fractional differential equations with p-Laplacian operator and an application to a waterborne disease model. Alexandria Engineering Journal, 70, 665-672.

[31] Agrawal, O. (2006). Fractional variational calculus and the transversality conditions. Journal of Physics A: Mathematical and General, 39(33), 10375.

[32] Bulut, H., & Ilhan, E. (2021). Fractional vector-borne disease model with lifelong immunity under Caputo operator. Physica Scripta, 96(8), 084006.

[33] Owolabi, K. M., Atangana, A., & Akgul, A. (2020). Modelling and analysis of fractal-fractional partial differential equations: application to reaction-diffusion model. Alexandria Engineering Journal, 59(4), 2477-2490.

[34] Al-Mdallal, Q. M., Hajji, M. A., & Abdeljawad, T. (2021). On the iterative methods for solving fractional initial value problems: new perspective. Journal of Fractional Calculus and Nonlinear Systems, 2(1), 76-81.

[35] Azil, S., Odibat, Z., & Shawagfeh, N. (2021). Nonlinear dynamics and chaos in Caputo-like discrete fractional Chen system. Physica Scripta, 96(9), 095219.

[36] Ullah, S., Zulfiqar, S., Buhader, A. A., & Khan, N. A. (2021). Analysis of Caputo-Fabrizio fractional order semi-linear parabolic equations via effective amalgamated technique. Physica Scripta, 96(3), 035214.

[37] Hu, C., Tian, Z., Wang, Q., Zhang, X., Liang, B., Jian, C., & Wu, X. (2022). A memristor-based VB2 chaotic system: Dynamical analysis, circuit implementation, and image encryption. Optik, 269, 169878.

[38] Jackiewicz, Z., Renaut, R., & Feldstein, A. (1991). Two-step runge–kutta methods. SIAM Journal on Numerical Analysis, 28(4), 1165-1182.

[39] Verner, J. H. (2006). Starting methods for two-step Runge–Kutta methods of stage-order 3 and order 6. Journal of computational and applied mathematics, 185(2), 292-307.

[40] Verner, J. H. (2006). Improved starting methods for two-step Runge–Kutta methods of stage-order p− 3. Applied numerical mathematics, 56(3-4), 388-396.

[41] Leng, X., Zhang, L., Zhang, C., & Du, B. (2023). Modeling and complexity analysis of a fractional-order memristor conservative chaotic system. Physica Scripta.

[42] Wang, S. F., & Ye, A. (2020). Dynamical Properties of Fractional-Order Memristor. Symmetry, 12(3), 437.

[43] Abro, K. A., & Atangana, A. (2021). Numerical study and chaotic analysis of meminductor and memcapacitor through fractal–fractional differential operator. Arabian Journal for Science and Engineering, 46, 857-871.

[44] Abro, K. A., Siyal, A., & Atangana, A. (2023). Strange Fractal Attractors and Optimal Chaos of Memristor–Memcapacitor via Non-local Differentials. Qualitative Theory of Dynamical Systems, 22(4), 156.

[45] Ertürk, V. S., & Momani, S. (2008). Solving systems of fractional differential equations using differential transform method. Journal of Computational and Applied Mathematics, 215(1), 142-151.

[46] Filali, D., Ali, A., Ali, Z., Akram, M., Dilshad, M., & Agarwal, P. (2023). Problem on piecewise Caputo-Fabrizio fractional delay differential equation under anti-periodic boundary conditions. Physica Scripta, 98(3), 034001.

[47] He, S., Wang, H., & Sun, K. (2022). Solutions and memory effect of fractional-order chaotic system: A review. Chinese Physics B, 31(6), 060501.

[48] Liu, X., Mou, J., Wang, J., Banerjee, S., & Li, P. (2022). Dynamical analysis of a novel fractional-order chaotic system based on memcapacitor and meminductor. Fractal and Fractional, 6(11), 671.

[49] Saadatmandi, A., & Dehghan, M. (2010). A new operational matrix for solving fractional-order differential equations. Computers & mathematics with applications, 59(3), 1326-1336.

[50] Yadav, L. K., Agarwal, G., & Kumari, M. (2020, December). Study of Navier-Stokes equation by using Iterative Laplace Transform Method (ILTM) involving Caputo-Fabrizio fractional operator. In Journal of Physics: Conference Series (Vol. 1706, No. 1, p. 012044). IOP Publishing.

[51] Abro, K. A., & Atangana, A. (2020). A comparative study of convective fluid motion in rotating cavity via Atangana–Baleanu and Caputo–Fabrizio fractal–fractional differentiations. The European Physical Journal Plus, 135(2), 1-16.

[52] Lin, H., Wang, C., Yu, F., Sun, J., Du, S., Deng, Z., & Deng, Q. (2023). A review of chaotic systems based on memristive Hopfield neural networks. Mathematics, 11(6), 1369.

[53] Petráš, I. (2020). Comments on “Chaotic oscillator based on memcapacitor and meminductor” (Nonlinear Dyn, DOI: 10.1007/s11071-019-04781-5). Nonlinear Dynamics, 102, 2945-2950.